Carcinogenesis vol.28 no.10 pp.2122–2130, 2007
doi:10.1093/carcin/bgm147
Advance Access publication July 5, 2007

Involvement of visinin-like protein-1 (VSNL-1) in regulating proliferative and invasive properties of neuroblastoma

Yi Xie[1], Hiuman Chan[1], Jianqing Fan[2], Yongxiong Chen[1], Joseph Young[1], Wen Li[1], Xiaoping Miao[1], Zhengwei Yuan[3], Huanmin Wang[4], Paul K.H.Tam[1] and Yi Ren[*,1,5]

[1]Department of Surgery, The University of Hong Kong, Hong Kong SAR, China, [2]Statistics Laboratory, Princeton University, Princeton, NJ, 08540 USA, [3]Department of Paediatric Surgery, The Second Affiliated Hospital of China Medical University, Shenyang, 110004 China, [4]Department of Paediatric Surgery, Beijing Children's Hospital, Capital University of Medical Sciences, Beijing, 100045 China and [5]Department of Cell Biology and Neuroscience, Rutgers University, Piscataway, NJ, 08854 USA

[*]To whom correspondence should be addressed. Tel: +732 445 2061;
Fax: +732 445 2063;
Email: ren@dls.rutgers.edu
Correspondence may also be addressed to Paul K.H. Tam. Tel: +852 2855 4580;
Fax: +852 2817 3155;
Email: paultam@hkucc.hku.hk

Tumor growth and metastasis require that tumor cells must have either the potential to shift genetically or epigenetically between proliferative and invasive phenotypes or both phenotypes simultaneously. In the present study, we demonstrated that neuroblastoma growth and invasion were distinct processes that were carried out by proliferative and invasive phenotypes of tumor cells, respectively. Two subpopulations from human neuroblastoma cell line were isolated: highly invasive (HI) cells and low-invasive (LI) cells. HI and LI cells had different proliferative rate and metastatic ability *in vitro* and *in vivo*. In addition, they had distinct activated signal pathways and sensitivities to chemotherapy drugs. Affymetrix microarray and quantitative reverse transcriptase–polymerase chain reaction revealed that visinin-like protein-1 (VSNL-1) mRNA in HI cells was significantly higher than that in LI cells. We also observed that VSNL-1 was over-expressed in tumor specimens from patients with distant organ metastases compared with those without metastases. Furthermore, the invasive and proliferative phenotypes of neuroblastoma cells could be exchanged by regulation of VSNL-1 expression *in vitro* and *in vivo*. Up-regulation of VSNL-1 potentiated the anoikis-resistant ability of neuroblastoma cell. The expression of anoikis inhibitor TrkB, intracellular adhesion molecule 1, major histocompatibility complex class I, CD44 and CD44v6 was associated with VSNL-1 level. These results suggested that distinct roles of proliferative and invasive phenotypes contributed to neuroblastoma progression and strongly demonstrated that VSNL-1 played a very important role in neuroblastoma metastasis.

Introduction

The ability of malignant tumors to metastasize is the major cause of death from cancer and failure of cancer treatment. Although the radical surgery treatment, radiotherapy and systemic chemotherapy are performed, the clinical outcome is unsatisfactory because of metastatic spread. It has been shown that tumor metastatic stage is one of the most important prognostic factors (1). Understanding the molecular mechanisms of the complex multistep process of tumor metastasis could facilitate the development of preventive measures, early diagnostic methods and better treatments.

Neuroblastoma is the most common extracranial solid tumor of childhood, and the hallmark of neuroblastoma is heterogeneity in both genotype and clinical behavior (2). Spontaneous regression and differentiation are common in infants and in early-stage tumors, whereas neuroblastoma is extremely aggressive in older children with late-stage tumors (3). Over 60% of neuroblastoma patients more than 1 year old have metastases at the time of diagnosis and show unfavorable outcomes (4). Little progress has been made in improving the poor prognosis of patients with late-stage neuroblastomas because metastasis is common. Most neuroblastomas metastasize to bone marrow and bone, some to lymph nodes, liver, lung and brain (5,6). However, very little is known about the mechanisms involved in metastases of neuroblastoma.

Tumor growth and metastasis require that tumor cells have either the potential to shift genetically or epigenetically between proliferative and invasive phenotypes or both phenotypes simultaneously. Thus, we hypothesized that heterogeneity of tumor phenotypes contributed to tumor development. In current study, we were able to isolate two subpopulations from human neuroblastoma cell line by transwell invasion chamber: highly invasive (HI) cells and low-invasive (LI) cells. Different properties of HI and LI cells were compared, and it was found that HI and LI cells were distinct in proliferation rate, metastatic ability, activated signal pathway and sensitivities to chemotherapeutic drugs. Visinin-like protein 1 (VSNL-1) was found to be involved in the regulation of the proliferative and invasive properties of neuroblastoma. VSNL-1 is expressed in the central nervous system, where it plays a crucial role in regulating cyclic adenosine 3′,5′-monophosphate levels, cell signaling and differentiation. Very little information is available regarding its roles in tumor development and metastasis. Our results indicate that VSNL-1 plays an important role in regulating tumor cell invasiveness and growth.

Abbreviations: DMEM, Dulbecco's modified Eagle's medium; ERK, extracellular signal-related kinase; FBS, fetal bovine serum; FITC, fluorescein isothiocyanate; FACS, fluorescence-activated cell sorting; HI, highly invasive; ICAM-1, intracellular adhesion molecule 1; i.v, intravenously; LI, low invasive; MHC-I, major histocompatibility complex class I; PBS, phosphate-buffered saline; p-Akt, phosphorylated-Akt; PI, propidium iodide; qRT–PCR, quantitative reverse transcriptase–polymerase chain reaction; s.c, subcutaneously; VSNL-1, visinin-like protein-1.

Materials and methods

Cells and cell culture

Neuroblastoma cell line SK-N-AS from American Type Culture Collection (Rockville, MD) was maintained in Dulbecco's modified Eagle's medium (DMEM; Life technologies, Grand Island, NY) supplemented with 10% fetal bovine serum (FBS, Life technologies).

Patient specimens

Neuroblastoma specimens were collected with informal consent from 16 patients at the Second Affiliated Hospital of China Medical University, and 6 patients at Queen Mary Hospital, the University of Hong Kong. Tumor specimens were obtained from patients with surgically resected primary neuroblastoma. The patients included 15 males and 7 females, and their median age at diagnosis was 48 months (range: 11–108 months). This study was approved by the Human Research Ethics Committee, Queen Mary Hospital, University of Hong Kong.

Isolation of HI and LI neuroblastoma cells

In order to isolate subclones with high migrating ability, transwell invasion chambers were used in this study as described by Kawamata *et al.* (7). Transwell assay was performed using cell culture insert with 8 μm pores (BD Falcon, Franklin Lakes, NJ). The surfaces of transwell were coated with 100 μl diluted Matrigel (BD Bioscience, Bedford, MA). Cells (5×10^4) in 500 μl DMEM with 1% FBS were seeded onto the top of the transwell filter and DMEM with 1% FBS were added to the bottom chamber of the transwell. After 24 h incubation, the cells in the upper and lower layers of the chamber were harvested and cultured. Clones derived from single cell by using a limiting dilution technique were selected and expanded into cell lines. Two subpopulations were isolated and referred as to LI cells and HI cells based on their different invasive ability.

Invasion assay

Transwell assay was also used to assess tumor cell invasion. After 24 h incubation, non-invading cells in the upper layers were swabbed off using a cotton-tipped swab and the invading cells in lower layers were fixed with 4% paraformaldehyde (Sigma-Aldrich, St. Louis, MO) for 10 min at room temperature, and then were rinsed in phosphate-buffered saline (PBS) and stained with 0.5% crystal violet (BDH Laboratory Supplies, Poole England) in 50% ethanol for 10 min at room temperature. The invading cells remained in the bottom side of the membrane were counted under microscope. All assays were performed in triplicate, and at least three independent experiments were performed.

3-[4,5-Dimethylthiazole-2-yl]-2,5-diphenyltetrazolium bromide assay

Cell proliferation was assessed using conversion of 3-[4,5-dimethylthiazole-2-yl]-2,5-diphenyltetrazolium bromide (Roche, Indianapolis, IN) into formazan product. Five thousand cells per well were seeded in 96-well plate and cultured for 48 h. 3-[4,5-Dimethylthiazole-2-yl]-2,5-diphenyltetrazolium bromide (0.5 mg/ml) was incubated with cells for 4 h and solubilization solution (100 μl/well) was added for overnight incubation. All the incubation was performed in humidified tissue culture incubator, 37°C, 5% CO_2 atmosphere. Absorbance was measured at 540 nm with background correction at 650 nm.

Tumor growth model

Male BALB/c nu/nu mice (5–6 weeks) were inoculated with 2×10^6 cells in 100 μl PBS subcutaneously (s.c.). Tumor dimensions were measured every 2 days using micrometer calipers. Tumor volumes were calculated using the following formula: Volume $= 1/2 \times a \times b^2$, where a and b represent the larger and smaller tumor diameters, respectively. All the animal experiments were approved by the Committee on the Use of Live Animals in Teaching and Research at the University of Hong Kong (Hong Kong, China).

Tumor metastatic model

Male BALB/c nu/nu mice (5–6 weeks) were injected with 2×10^6 cells in 100 μl PBS intravenously (i.v.). The nude mice were killed 3 months later and evaluated the tumor formation in the lung or bone marrow. The lungs were excised and fixed with 4% formalin for hematoxylin and eosin staining. To detect the tumors in the bone marrow, both the forelimbs and hind limbs were separated from the bodies at the joints. Bone marrow was collected and washed once with PBS before being cultured in six-well plate using DMEM with 10% FBS. Non-adhesion cells were washed away with PBS after overnight incubation. Human neuroblastoma cells were identified by fluorescence-activated cell sorting (FACS) analysis (Becton Dickinson, Mountain View, CA) using a fluorescein isothiocyanate (FITC)-conjugated anti-human major histocompatibility complex class I (MHC-I) antibody (BD pharmingen, San Diego, CA).

Green fluorescence protein-actin and DsRed2-Nuc transfection

In order to label LI and HI cells with different colors, the plasmids pEGFP-actin (BD Biosciences, Palo Alto, CA) and pDsRed2-Nuc (BD Biosciences, Palo Alto, CA) were transfected into LI and HI cells, respectively. In brief, 5 μg of plasmid DNA was mixed with 10 μl Lipofectamine 2000 (Invitrogen, Carlsbad, CA) in 500 μl DMEM and incubated for 20 min at room temperature. The mixture was added to 90% confluent cells in six-well plates, which were then incubated for 24 h at 37°C under 5% CO_2 atmosphere. Transfected cells were then incubated in the presence of 800 μg/ml of G418 (BD Clontech, Palo Alto, CA) to select positive clones.

Affymetrix GeneChip

Total RNA samples were extracted with the TRIzol reagent (Invitrogen) according to the manufacturer's instructions. Probe synthesis and hybridization of human U-133A GeneChip Oligo Microarrays (Affymetrix, Santa Clara, CA) were performed in accordance with the manufacturer's instructions. Gene expression data (CHP file of Affymetrix Microarray Suite 5.0 software) were normalized to a global target intensity of 500.

Real-time quantitative reverse transcriptase–polymerase chain reaction

Total RNA was extracted from cells using Trizol reagent (Invitrogen) or from paraffin-embedded tissue using RecoverALL™ Total Nucleic Acid Isolation Kit (Ambion, Austin, TX). cDNA is synthesized using random hexamer (Invitrogen). Real-time quantitative polymerase chain reaction (PCR) is performed according to the instruction described in ABI assay-on-demand VSNL kit (Applied Biosystem, Foster City, CA). Values were obtained from the Ct number at which the increase in signal associated with exponential growth of PCR products was first detected. According to the manufacturer's manual, 18S was chosen as an endogenous control for cells and PGP9.5 for patient specimens. Results were expressed as n-fold differences in target gene expression relative to endogenous control (n_{target}). In brief, they were determined by the formula $n_{\text{target}} = 2^{\Delta\Delta Ct}_{\text{sample}}$, where the ΔΔCt was determined by subtracting the ΔCt value of the control gene from that of the target gene, and the ΔCt value was determined by subtracting the average Ct value of the control gene from that of the target gene. The n_{target} values of samples were normalized such that the value of the control group was 1. Experiments were performed with duplicates for each data.

VSNL-1 cDNA transfection

The cDNA of VSNL-1 was ligated in the modified plasmid pSec/His tagged with His. Cells were transfected using Lipofectamine 2000 as the manufacturer's instruction. To establish VSNL-1 expression, stable clones and vector control lines, cells transfected with pSec-VSNL-1 or vector alone were diluted in 1:5 after 24 h transfection and then incubated and positive clones were selected in the presence of 400 μg/ml of hygromycine B (BD).

Western blotting

Cells were lysed in RIPA buffer [0.5% sodium deoxycholate, 0.1% sodium dodecyl sulfate (SDS), 1% Nonidet-P40 and PBS] with phenylmethanesulfonyl fluoride and protease inhibitors (Roche, Diagnostics, Mannheim, Germany) for 30 min on ice. The protein concentrations were determined by the Bio-Rad DC assay (Bio-Rad, Hercules, CA). The samples were adjusted to equal protein concentrations and subjected to sodium dodecyl sulfate–polyacrylamide gel electrophoresis. Proteins on the gel were transferred onto nitrocellulose membranes (Millipore, Bedford, MA), then were blocked with 5% bovine serum albumin in Tris-buffered saline containing 0.1% Tween 20 for 1 h at room temperature. The membranes were incubated with the anti-His antibody (Invitrogen) overnight at 4°C. After being washed with Tris-buffered saline containing 0.1% Tween 20, the membranes were incubated with the appropriate horseradish peroxidase-conjugated secondary antibody (DAKO, Glostrup Denmark). The immunoreactive bands were visualized with ECL kit (Amersham Pharmacia Biotech, Buckinghamshire, UK).

Anoikis assay

Anoikis levels were measured using a protocol modified from Park *et al.* (8). Cells (4×10^5) were seeded in 60 mm corning petri dishes (Sigma-Aldrich), cultured in DMEM with 10% FBS and 400 μg/ml hygromycin B. After 48 h incubation, apoptosis were detected by FITC–annexin V/propidium iodide (PI) double staining (Roche, IN). After washing twice with PBS, cells were labeled with FITC–annexin V and PI for 10 min in the dark at room temperature, and then cellular fluorescence was measured with FACScan flow cytometer (Becton Dickinson).

FACS analysis

Cells were processed for single staining with phycoerythrin-conjugated intracellular adhesion molecule 1 (ICAM-1), FITC-conjugated MHC-I or monoclonal antibodies against CD44, CD44v6 and TrkB, followed by FITC-labeled goat anti-mouse antibody specific for IgG. Fluorescence acquisition was done on FACScan flow cytometer. All antibodies were from R&D (Minneapolis, MN) except monoclonal antibody against CD44 (DAKO, Denmark).

Statistical analysis

Statistical tests including the Mann–Whitney U, χ^2 and Kendall tau-b tests were used. A P value of less than 0.05 indicated that the difference was significant. All statistical analyses were performed using the computer software Statistical Package for the Social Sciences 10.0 (SPSS Inc., Chicago, IL).

Results

Isolation of subpopulations with different proliferative property and metastatic potential

Transwell chamber has been used to measure and isolate tumor cells with different invasive property (7,9). Therefore, we applied it to isolate tumor cells with HI phenotype. Two subpopulations with different invasive ability were isolated from neuroblastoma cell line SK-N-AS: HI cells and LI cells. The migration of HI cells was significantly faster than LI cells (Figure 1A).

We further examined HI and LI cells for proliferative properties *in vitro* and *in vivo*. The *in vitro* data showed that LI cells grew significantly faster than HI cells, assessed by 3-[4,5-dimethylthiazole-2-yl]-2,5-diphenyltetrazolium bromide and cell counting (Figure 1B and C, $P < 0.01$). We also inoculated HI and LI cells s.c. into athymic nude mice and compared the rates of tumor growth (Figure 1D). LI xenografts grew significantly faster than HI xenografts. The tumor volume of LI was nearly five times than that of the HI xenografts by 32 days of growth ($P < 0.01$).

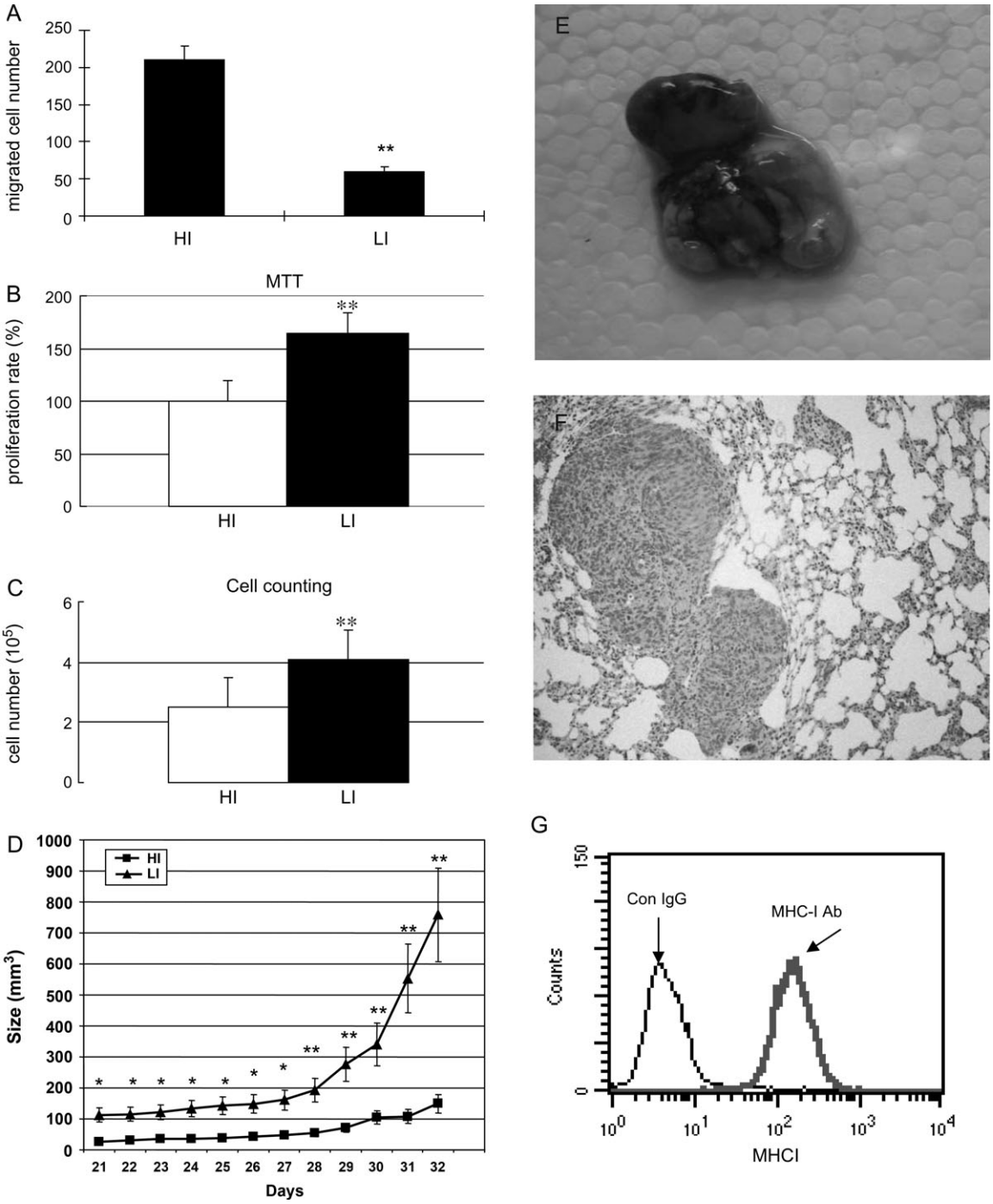

Fig. 1. Migration and proliferative properties of HI and LI cells *in vitro* and *in vivo*. (**A**) Migration of HI and LI cells assessed by transwell invasion chamber. (**B** and **C**) HI and LI cells were cultured in 96-well plate for 48 h. Proliferative rate was evaluated by 3-[4,5-dimethylthiazole-2-yl]-2,5-diphenyltetrazolium bromide assay (B) and cell counting (B). The data were expressed as mean ± SD ($^{**}P < 0.01$). (**D**) Neuroblastoma growth curve in nude mice. Nude mice were injected s.c. with HI and LI cells cells (2×10^6 cells in 100 μl PBS), respectively. Tumor development was followed to 32 days. Values are mean ± SD ($n = 10$, $^{*}P < 0.05$, $^{**}P < 0.01$). (**E–G**) Metastatic properties of HI and LI cells *in vivo*. Nude mice were injected with HI and LI cells (2×10^6 cells in 100 μl PBS) *i.v.* The nude mice were killed 3 months later and evaluated the tumor formation in the lung or bone marrow. (D) The representative metastatic neuroblastomas in the lung. (E) H&E staining of the tumor cells in the lung. (F) Human MHC-I-positive tumor cells were detected in the bone marrow of nude mice.

Burchill *et al.* (10) were able to detect neuroblastoma cells in peripheral blood, suggesting its hematogenous dissemination. Therefore, i.v. injection of neuroblastoma cells into mice could be a murine model to investigate neuroblastoma metastasis (11). We administrated HI and LI cells into athymic nude mice i.v. After 3 months of the injection, 76.9% mice injected with HI cells developed lung metastasis (Figure 1E) and 23.1% had bone marrow metastasis, whereas only 18.2% mice developed lung metastasis and none had bone marrow metastasis in mice injected with LI cells (Table I) ($P < 0.05$). Histological examination indicated tumor cells in the lung (Figure 1F). FACS analysis showed that isolated cells from mice bone marrow were human MHC-I positive, suggesting bone marrow metastasis (Figure 1G).

To further confirm that HI and LI cells have distinct properties for proliferation and metastasis, HI and LI cells were transfected with pDsRed2-Nuc vector and pEGFP-actin vector, respectively.

pDsRed2-Nuc labeled the nucleus of HI cells with red fluorescence and pEGFP-actin labeled the actin cytoskeleton in LI cells with green fluorescence. The equal numbers of HI and LI cells (1×10^6 cells) were mixed and then inoculated into nude mice s.c. and allowed to grow over a period of 30 days followed. The HI and LI mixture was also injected to mice i.v. to establish metastatic model as described previously and mice were killed after 3 months injection. The tumor growing in local sites and metastatic lung nodules were prepared in frozen section and then investigated under fluorescent microscope. The results showed that majority of cells in lung were HI cells labeled with red fluorescence. In contrast, tumor formed quickly in the local sites of s.c. injection and majority of cells were LI cells labeled with green fluorescence (Figure 2). These data further confirmed that HI cells had HI potential but grew slower, whereas LI had higher proliferative capacity but their invasive potential was poor.

Differences in signaling pathways of HI and LI cells

In order to investigate whether different signaling pathways contribute to the different phenotypes, we evaluated the signaling pathways in HI and LI cells. Higher levels of phosphorylated-Akt (p-Akt) at Ser 473 were detected in LI cells and there were similar levels of p-Akt at Thr 308 in both HI and LI cells. In contrast, p-Akt in HI cells was weak positive. On the other hand, p-44/42 were positive on both HI and LI cells (Figure 3A). These data may suggest that activation of extracellular signal-related kinase (ERK) is associated with both proliferation and invasion in neuroblastoma cells, whereas activation of Akt is correlated with the proliferative phenotype.

Different responsiveness to chemotherapy of HI and LI cells

Vincristine, adriamycin, cyclophosphamide, cisplatinum and VP-16 are commonly used as chemotherapy drugs for neuroblastoma. Therefore, we assessed the responsiveness of HI and LI cells to these drugs on cell proliferation. VP16- and adriamycin-induced growth inhibitory effects occurred in HI with IC_{50} values 1000 and 12.0 ng/ml, respectively. However, the effects of VP16 and adriamycin on LI cells were less when compared with HI cells: IC_{50} values for both drugs were >10000 and 100 ng/ml, respectively ($P < 0.01$). The sensitivities of HI and LI cells to cyclophosphamide and vincristine were almost the same (Figure 3B). Similar results were observed in the cells treated with cisplatinum (data not shown). All these data illustrated that HI and LI had different responsiveness to certain drugs.

Table I. Different metastatic potential between HI and LI cells *in vivo*

	Lung metastasis	Bone marrow metastasis
HI cells	10/13 (76.9%)*	3/13 (23.1%)*
LI cells	2/11 (18.2%)	0/10 (0)

*$P < 0.05$.

VSNL-1 over-expression in HI cells and patients with distant organ metastasis

To better understand the molecular mechanisms of HI and LI cells in the development of neuroblastoma, Affymetrix microarray and quantitative reverse transcriptase–PCR (qRT–PCR) were applied to identify genes whose expression was different in these two types of cells. Affymetrix microarray showed that of a total of about 22 283 probe sets, 14 genes were found to be statistically significant and highly differentially expressed between HI and LI cells ($P < 0.05$). VSNL-1, *c-met* and integrin α4, which are associated with tumor metastasis, were highly expressed in HI cells compared with LI cells. The qRT–PCR data showed that the mRNA level of VSNL-1 in HI cells was about 10 times higher than that of LI cells ($P < 0.01$) (Figure 3C), whereas the expression of *c-met* and integrin α4 in HI was 1.97 and 1.98 times higher compared with LI cells (data not shown).

As Affymetrix microarray revealed that VSNL-1 was differentially expressed in HI and LI cells ($P < 0.05$), we undertook qRT–PCR to confirm this founding. We further studied the association of VSNL-1 and metastatic status in neuroblastoma specimens from patients by qRT–PCR. A total of 22 neuroblastoma patients' specimens were examined for expression of VSNL-1 mRNA. It was found that the mRNA level of VSNL-1 was significantly correlated with the clinical stage. VSNL-1 mRNA in stage IV patients was over 13 times higher than stage I patients ($P < 0.05$) (Figure 3D), suggesting that overexpression of VSNL-1 was correlated with tumor metastasis.

Function of VSNL-1 on neuroblastoma cells

To investigate the function of VSNL-1 on neuroblastoma cells, the VSNL-1 cDNA withswas transfected into LI cells that had lower VSNL-1 expression. Western blot analysis showed that the VSNL-1 detected by anti-His antibody was positive in clone A and B transfected with VSNL-1 cDNA, whereas it was not expressed in cells transfected with vector alone (Figure 4A).

We further evaluated the proliferative effect of VSNL-1 transfection and found that VSNL-1 transfection into LI cells inhibited neuroblastoma cell proliferation *in vitro*. The proliferation rate of VSNL-1

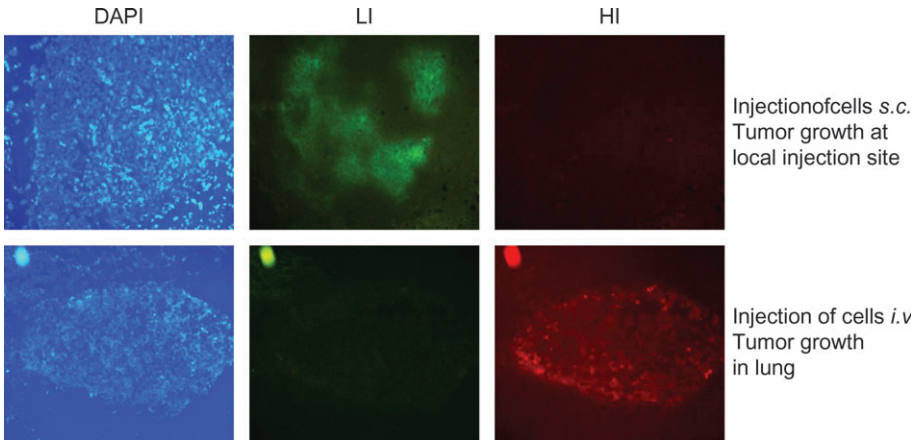

Fig. 2. Tumor growth in lung and injection sites. HI cells were labeled with red fluorescence, whereas LI cells with green fluorescence. The equal numbers of HI and LI cells (1×10^6 cells) were mixed and then inoculated into nude mice s.c. and allowed to grow over a period of 30 days followed. The HI and LI mixture was also injected to mice *i.v.* and mice were killed after 3 months injection. The tumor grown in local sites and metastatic lung nodules were prepared in frozen section and then investigated under fluorescent microscope. Majority of cells in lung were HI cells labeled with red fluorescence. Tumor formed in the local sites of s.c. injection after 30 days injection and majority of cells were LI cells labeled with green fluorescence.

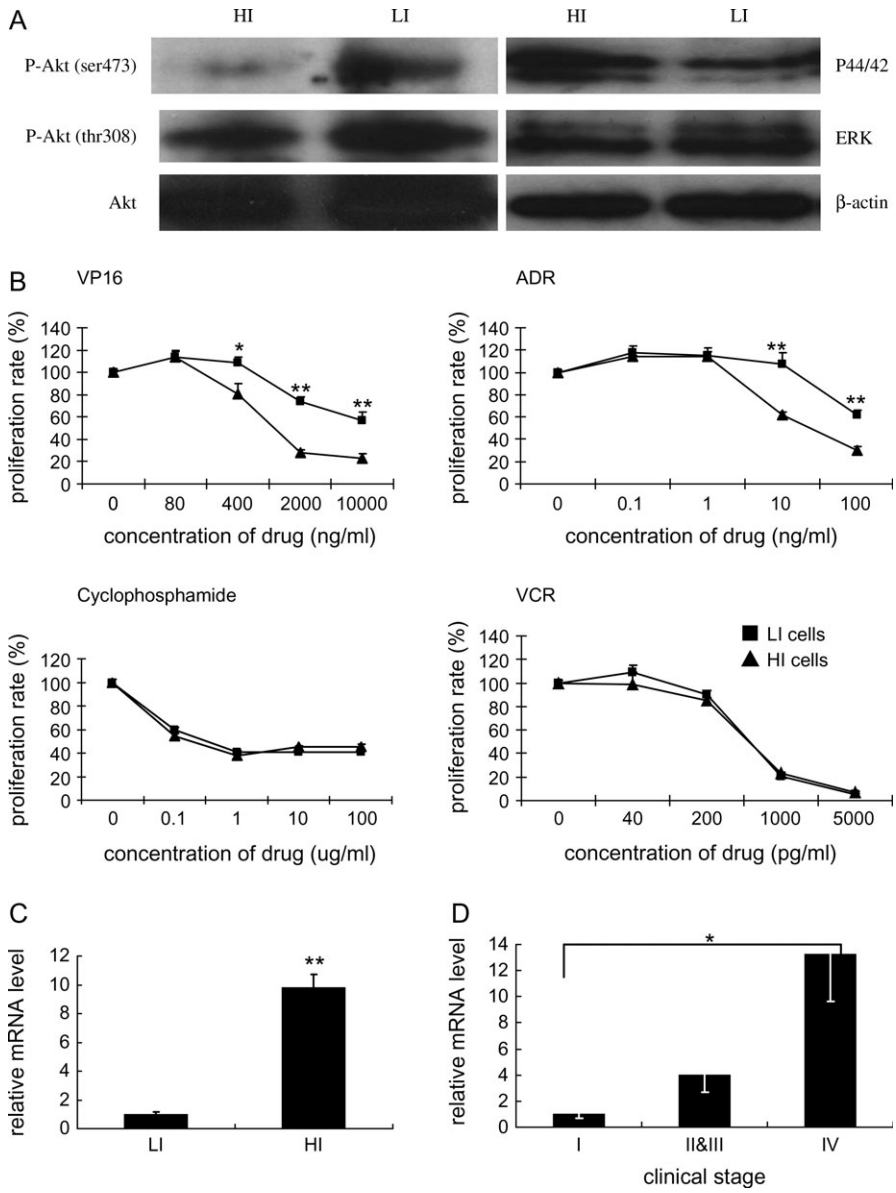

Fig. 3. Different characteristics of HI and LI cells. (**A**) Signal pathways of HI and LI cells detected by Western blot analysis. (**B**) Proliferative effects of chemotherapeutic drugs on HI and LI cells evaluated by MTT assay. Cells were cultured with VP-16, adriamycin (ADR), cyclophosphamide and vincristine (VCR) for 72 h in 96-well plate. Each treatment group contained 8 replicates. The data were expressed as mean ± SD and similar results were obtained from three independent experiments ($^{*}P < 0.05$, $^{**}P < 0.01$). (**C** and **D**) Association of VSNL-1 with neuroblastoma invasive property. (C) The levels of VSNL-1 mRNA in HI and LI cells detected by qRT–PCR. The data were expressed as mean ± SD, and similar results were obtained from three independent experiments ($^{**}P < 0.01$) (D) VSNL-1 mRNA in neuroblastoma patients' specimens detected by qRT–PCR ($^{*}P < 0.05$, stage I: $n = 7$; stage II and III: $n = 7$; stage IV: $n = 8$).

tranfectants was less than 80% (74 ± 2.3%) compared with vector-alone transfectants ($P < 0.05$) (Figure 4B). *In vivo* experiment also showed that VSNL-1 transfection into LI cells significantly slowed tumor growth in nude mice (Figure 4C).

We also assessed whether the invasive capacity could be changed by modifying expression of VSNL-1. LI cells transfected with VSNL-1 cDNA acquired capacity for invasion (Figure 4D). After 3 months injection of LI cells transfected with VSNL-1 cDNA (i.v.), six of 10 mice developed lung metastasis and one of 10 developed bone marrow metastasis, whereas only three of 10 mice injected with LI cells transfected with vector alone developed lung nodules and none of them developed bone marrow metastasis ($P < 0.05$)(Table II).

Effects of VSNL-1 on anoikis

Aniokis assay was measured using corning petri dishes that could prohibit cell attachment. LI cells transfected with VSNL-1 or vector alone were seeded on the dish. After 48 h incubation with DMEM plus 10% FBS and hygromycin B (400 μg/ml), cell apoptosis were detected by PI and annexin V double staining. In all, 74.43% of VSNL-1 transfectants were annexin V and PI negative. In contrast, only 27.71% of vector-alone transfectants were annexin V and PI negative ($P < 0.05$) (Figure 5A). The data illustrated that up-regulation of VSNL-1 increased the resistance of neuroblastoma cells to anoikis which was an important step in the process of metastasis.

Effects of VSNL-1 on the expression of metastasis-related proteins

We next investigated whether other metastasis-related molecules could be regulated by VSNL-1. VSNL-1 transfectants expressed higher level of anoikis inhibitor, TrkB (11, 12), compared with vector-alone transfectants. In addition, VSNL-1 transfection down-regulated the expression of ICAM-1, MHC-I, CD44 and CD44v6 (Figure 5B).

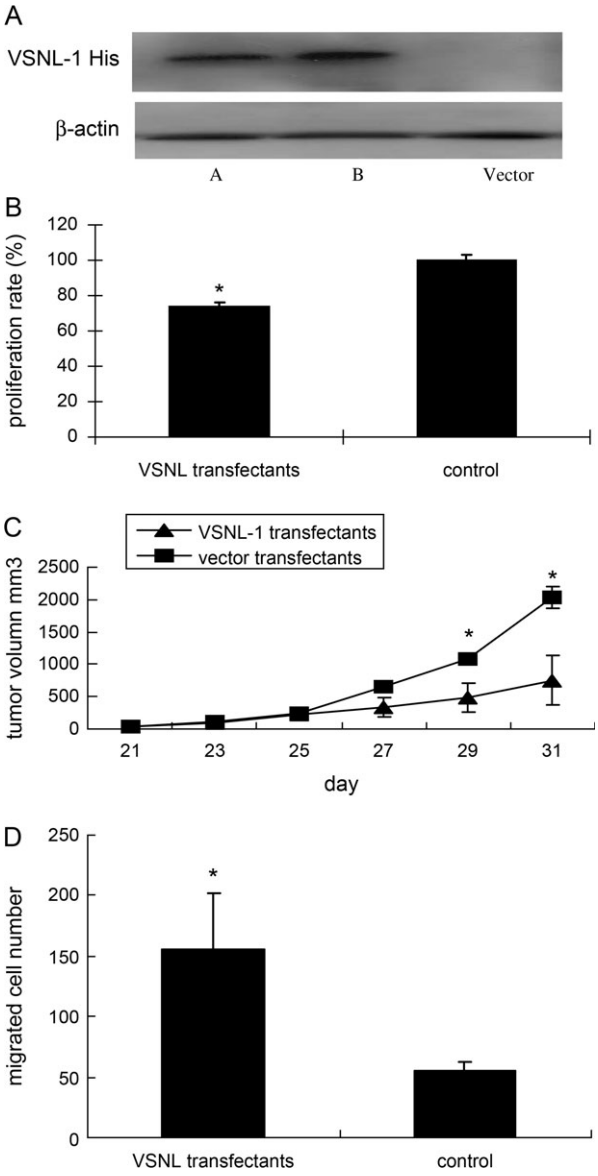

Fig. 4. Function of VSNL-1 in neuroblastoma proliferation and invasion. (**A**) The expression of VSNL-1 in VSNL-1-transfected LI cells (clones A and B) and vector-alone transfectants detected by anti-His antibody. (**B–D**) Proliferative effects and invasive property of cells transfected with VSNL-1 or vector alone. (B) LI cells transfected with VSNL-1 cDNA and vector alone (control) were cultured in 96-well plate for 48 h. Proliferative rate was evaluated by 3-[4,5-dimethylthiazole-2-yl]-2,5-diphenyltetrazolium bromide assay. The data were expressed as mean ± SD and similar results were obtained from three independent experiments ($^*P < 0.05$). (C) Effect of VSNL-1 on neuroblastoma growth *in vivo*. Nude mice were injected s.c. with LI cells transfected with VSNL-1 cDNA and vector alone (2×10^6 cells in 100 μl PBS). Tumor development was followed to 31 days. Values are means SD($n = 10$, $^*P < 0.05$). (D) VSNL-1 transfection enhances the invasion of tumor cells assessed by transwell invasion chamber. The data were expressed as mean ± SD and similar results were obtained from three independent experiments ($^*P < 0.05$).

Discussion

Despite intensive investigations, the fundamental rule of tumor initiation and metastasis in neuroblastoma remains elusive. In the present study, we demonstrated that the growth and invasion of neuroblastoma were distinct processes that were carried out by proliferative and invasive phenotypes of tumor cells, respectively. These tumor cells with distinct properties not only had different response to chemo drugs but also activated distinct signaling pathways. Furthermore, the invasive and proliferative phenotypes of neuroblastoma cells could be exchanged by regulation of VSNL-1 expression. Our data showed that HI cells grew slower *in vitro* and *in vivo*. These results are consistent with the previous reports that human melanoma high metastatic line had more significant decrease in proliferation *in vitro* compared with the low metastatic line from the same parental line (13). It is also demonstrated that metastatic glioblastoma cells have low proliferative state (14). Our finding may help to explain why metastatic tumor growth starts just to be detected even after local tumors are resected for a long period of time. Metastatic tumor cells from *in situ* tumor have been already in circulation or distance organs but they are not detectable in the early stage as they have lower proliferative rate. Once metastatic tumor cells seed in organs, the invasive phenotype may be changed to proliferative phenotype, and therefore, metastatic tumors start to grow. However, this hypothesis requires further study.

Table II. Enhancement of the metastatic potential of neuroblastoma cells by VSNL-1 cDNA transfection

	Lung metastasis	Bone marrow metastasis
VSNL-1 transfectants	6/10 (60.0%)*	1/10 (10.0%)*
Vector-alone transfectants	3/10 (30.0%)	0/10 (0)

*$P < 0.05$.

Understanding the molecular phenotypic determinants of tumor heterogeneity is essential in assessing therapeutic outcomes in the management of tumor progression. Akt is over-expressed or continuously activated in tumor cells (15) such as neuroblastoma, making them resistant to apoptosis induced by chemotherapeutic drugs (16). Akt inhibitors sensitize human neuroblastoma cells to chemotherapy (16). Activation of mitogen-activated protein kinase /ERK in tumors enhanced both proliferation and invasion (17). We found that higher levels of active Akt at serine 473 (S473) were detected in LI cells and it was weak positive in HI cells, whereas there is no difference in the levels of p-Akt at threonine 308, indicating that different upstream kinases are involved in. On the other hand, p-44/42 ERK was positive on both HI and LI cells. Our data support the idea that activation of Akt mediates proliferation, whereas ERK pathway controls both proliferation and invasion in neuroblastoma cells. We also showed that LI cells, which had higher level of p-Akt, were more resistant to chemotherapy. These results suggested that different phenotypes or signaling pathways might result in the distinct responsiveness to chemotherapy. Therefore, multiple signaling pathways may need to be targeted for maximal therapeutic efficacy.

Tumors are heterogeneous with respect to metastatic potential (18). Investigation of tumor cells with different metastatic property and identification of genes implicated in the control of metastases are important to understand the metastatic mechanisms, find biomarkers and new methods of intervention. In current study, we found that the level of VSNL-1 in HI cells was significantly higher compared with LI cells and expression of VSNL-1 in tumor specimens was significantly correlated with patients' clinical stages (metastatic status). VSNL-1 in Stage IV patients with distant organ metastasis was over 13 times higher than in stage I patients. Furthermore, the invasive capacity of neuroblastoma cells could be enhanced *in vitro* and *in vivo* by increase of VSNL-1 expression, suggesting that VSNL-1 was one of the key factors that controlled the turnover of neuroblastoma proliferative and invasive phenotypes. The tumor formation in the lung and bone marrow resulted from the higher metastatic property of neuroblastoma cells but not from the higher proliferative ability of cells. However, Mahloogi *et al.* found that the VSNL-1 expression in esophageal squamous carcinoma was reversely correlated with tumor invasive features, which may due to VSNL-1 elevated the intracellular cyclic adenosine 3′,5′-monophosphate level (19). The elevation of cyclic adenosine 3′,5′-monophosphate play both positive (20) and negative role (21) in cell migration. The precise

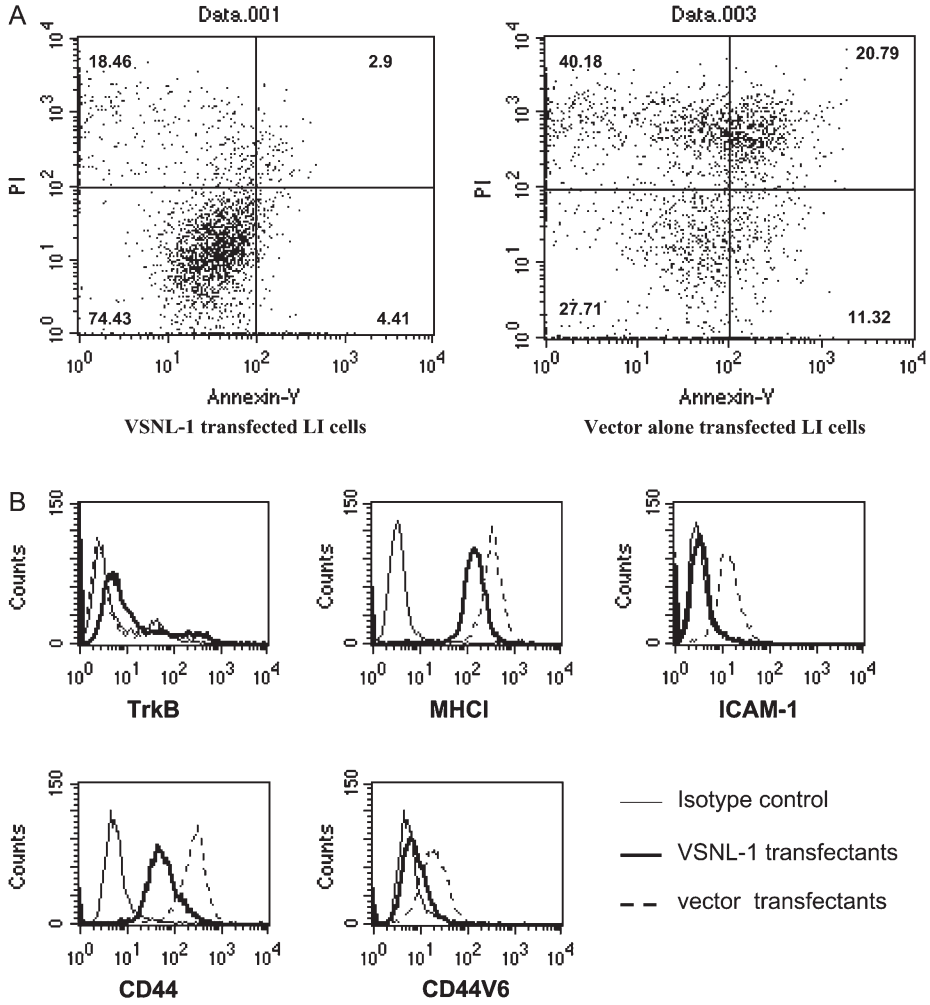

Fig. 5. Effects of VSNL-1 on cell anoikis and expression of metatasis-related molecules (**A**) Anoikis of LM cells transfected with VSNL-1 and vector alone. Results were representative of three experiments. (**B**) The expression of metastasis-related proteins on LM cells transfected with VSNL-1 and vector alone. Cells were labeled with antibodies against TrkB, MHC-I, ICAM-1, CD44 and CD44V6. Results were representative of three experiments.

functions of VSNL-1 have not been clarified, and this protein probably plays different roles in squamous carcinoma and neuroblastoma.

Metastasis is a multi-step process that includes the invasion of adjacent tissues, intravasation, and transportation through the circulatory system, arrest at a secondary site, extravasation and growth in a secondary organ. The events subsequent to entering circulation are rate limiting in the process (9). Anoikis, meaning ''homeless'' in Greek words, is defined as a phenomenon reflecting tumor cell apoptosis because of loss of adhesion. Resistance to anoikis contributes to metastasis by increasing cells viability after they loss the cell-cell and cell-extracellular matrix contacts (22). Our data showed that up-regulation of VSNL-1 inhibited the anoikis of neuroblastoma cells. We also found that over-expression of VSNL-1 up-regulated the expression of TrkB. TrkB over-expression in neuroblastoma is strongly associated with *MYCN* amplification (23), which is an reliable marker for poor outcome of neuroblastoma patients (24). TrkB has been reported recently as an inhibitor of anoikis (16). Additionally, TrkB confers an enhanced malignant phenotype to the neuroblastoma cells (26). Our data showed that the expression of TrkB was correlated positively with expression of VSNL-1. Therefore, we reasoned that VSNL-1 might inhibit neuroblastoma cell anoikis and enhance the cell invasion through up-regulating the expression of TrkB.

It is well documented that down-regulation of MHC-I and ICAM-1 contributes to tumor metastasis. Down-regulation of MHC-I helps tumor cells evade from T cell-mediated immune response (26). Lower expression of MHC-I is found in metastatic cervical carcinoma, melanoma and head and neck squamous cell carcinoma compared with primary tumors (27–29). In neuroblastoma, the *MYCN* amplification suppresses the MHC-I expression (30). It is consequently deduced that neuroblastoma patients with poor prognosis express lower MHC-I when considering the correlation of *MYCN* amplification with patients' outcome. ICAM-1 is a cell-surface glycoprotein belonging to the immunoglobulin superfamily (31). Lower ICAM-1 expression was observed in metastatic gastric cancer, esophageal cancer, colorectal cancer and breast cancer (32–36). In respect of neuroblastoma, ICAM-1 only expresses on a minority of clinical specimens that are MYCN negative, and this subset of tumors have a better prognosis (37). Patients with low-expression ICAM-1 and MHC-I have higher risk of tumor relapse than those with either low level of ICAM-1 or MHC-I (33). Expression of ICAM-1 and MHC-I is more frequent on low-stage neuroblastomas as compared with metastatic stage IV neuroblastomas (34,38). Neuroblastoma with low expression of ICAM-1 showed less susceptible to MHC unrestricted nature killer NK and lymphokine-activated killer cells (39). Up-regulation of ICAM-1 can partially explain the increased susceptibility to lymphokine-activated killer-, monocyte- and NK-mediated lysis (40–42). All these findings suggested that ICAM-1 and MHC-I might have synergetic role in immune response of neuroblastoma cells. In this study, VSNL-1 transfection simultaneously down-regulated MHC-I and ICAM-1 expression in neuroblastoma cells, which might contribute to the higher

metastatic potential by increasing the ability to evade from immune surveillance.

CD44 is a transmembrane glycoprotein that mediates cell–cell and cell–cell extracellular matrix adhesion (43). Over-expression of CD44 and its isoforms are correlated with tumor progression and metastasis in many human cancers including non-Hodgkin's lymphoma (44), gastric carcinoma (45), colorectal carcinoma (46) and brain tumor (47). However, low level or loss of CD44 expression is associated with progression and metastasis in neuroblastoma (48), prostate cancer (49) and bladder transitional cell carcinoma (50). These studies suggest that the relationship between CD44 expression and the occurrence of metastasis is tumor specific. Higher CD44 expression in neuroblastoma is found in low-stage and stage IV tumors (neuroblastomas in infants less than 1 year with dissemination limited to skin, liver and/or bone marrow. Stage IV neuroblastomas usually undergo spontaneous maturation and regression), whereas repressed CD44 expression is found in stage IV tumors with *MYCN* amplification (46,51). Some studies reported that high expression of CD44V6 is a predictor of metastasis in colon cancer (52) and gastric cancer (53). In contrast, metastasis progression correlates with down-regulation of CD44V6 in prostate cancer (54). In this study, we have showed that up-regulation of VSNL-1 decreased the expression of CD44 and CD44V6 which might also contribute to neuroblastoma metastasis.

Taken together, our study findings demonstrated that distinct roles of proliferative and invasive phenotypes contribute to neuroblastoma progression and strongly suggested that VSNL-1 enhanced neuroblastoma cell invasion and metastasis through regulation of TrkB, MHC-I, ICAM-1 and CD44.

Funding

Hong Kong Research Grants Council (HKU 7250/02M) and NIH grant R01-GM072611.

Acknowledgements

Conflict of Interest Statement: None declared.

References

1. Jiang,Z. *et al*. (2006) Analysis of RNA-binding protein IMP3 to predict metastasis and prognosis of renal-cell carcinoma: a retrospective study. *Lancet Oncol.*, **7**, 556–564.
2. Brodeur,G.M. (2003) Neuroblastoma: biological insights into a clinical enigma. *Nat. Rev. Cancer*, **3**, 203–216.
3. Pritchard,J. *et al*. (1994) Why does stage 4s neuroblastoma regress spontaneously? *Lancet*, **344**, 869–870.
4. Cotterill,S.J. *et al*. (2000) Clinical prognostic factors in 1277 patients with neuroblastoma: results of The European Neuroblastoma Study Group 'Survey' 1982–1992. *Eur. J. Cancer*, **36**, 901–908.
5. DuBois,S.G. *et al*. (1999) Metastatic sites in stage IV and IVS neuroblastoma correlate with age, tumor biology, and survival. *J. Pediatr. Hematol. Oncol.*, **21**, 181–189.
6. Cowie,F. *et al*. (1997) Lung involvement in neuroblastoma: incidence and characteristics. *Med. Pediatr. Oncol.*, **28**, 429–432.
7. Kawamata,H. *et al*. (2003) Identification of genes differentially expressed in a newly isolated human metastasizing esophageal cancer cell line, T.Tn-AT1, by cDNA microarray. *Cancer Sci.*, **94**, 699–706.
8. Park,M.Y. *et al*. (1999) Apoptosis induced by inhibition of contact with extracellular matrix in mouse collecting duct cells. *Nephron*, **83**, 341–351.
9. McClatchey,A.I. (1999) Modeling metastasis in the mouse. *Oncogene*, **18**, 5334–5339.
10. Burchill,S.A. *et al*. (2001) Circulating neuroblastoma cells detected by reverse transcriptase polymerase chain reaction for tyrosine hydroxylase mRNA are an independent poor prognostic indicator in stage 4 neuroblastoma in children over 1 year. *J. Clin. Oncol.*, **19**, 1795–1801.
11. Iwakawa,M. *et al*. (1994) A murine model for bone marrow metastasis established by an i.v. injection of C-1300 neuroblastoma in A/J mice. *Clin. Exp. Metastasis*, **12**, 231–237.
12. Douma,S. *et al*. (2004) Suppression of anoikis and induction of metastasis by the neurotrophic receptor TrkB. *Nature*, **430**, 1034–1039.
13. Ormerod,E.J. *et al*. (1989) Different growth responses to agents which elevate cAMP in human melanoma cell lines of high and low experimental metastatic capacity. *Clin. Exp. Metastasis*, **7**, 85–95.
14. Gao,C.F. *et al*. (2005) Proliferation and invasion: plasticity in tumor cells. *Proc. Natl Acad. Sci. USA*, **102**, 10528–10533.
15. Toker,A. *et al*. (2006) Akt signaling and cancer: surviving but not moving on. *Cancer Res.*, **66**, 3963–3966.
16. Ho,R. *et al*. (2002) Resistance to chemotherapy mediated by TrkB in neuroblastomas. *Cancer Res.*, **62**, 6462–6466.
17. Handra-Luca,A. *et al*. (2003) Extra-cellular signal-regulated ERK-1/ERK-2 pathway activation in human salivary gland mucoepidermoid carcinoma: association to aggressive tumor behavior and tumor cell proliferation. *Am. J. Pathol.*, **163**, 957–967.
18. Weiss,L. (2000) Metastasis of cancer: a conceptual history from antiquity to the 1990s. *Cancer Metastasis Rev.*, **19**I–XI, 193–383.
19. Mahloogi,H. *et al*. (2003) Overexpression of the calcium sensor visinin-like protein-1 leads to a cAMP-mediated decrease of *in vivo* and *in vitro* growth and invasiveness of squamous cell carcinoma cells. *Cancer Res.*, **63**, 4997–5004.
20. Plopper,G.E. *et al*. (2000) Antibody-induced activation of beta1 integrin receptors stimulates cAMP-dependent migration of breast cells on laminin-5. *Mol. Cell Biol. Res. Commun.*, **4**, 129–135.
21. Whelan,M.C. *et al*. (2003) Collagen I initiates endothelial cell morphogenesis by inducing actin polymerization through suppression of cyclic AMP and protein kinase A. *J. Biol. Chem.*, **278**, 327–334.
22. Frisch,S.M. *et al*. (1994) Disruption of epithelial cell-matrix interactions induces apoptosis. *J. Cell Biol.*, **124**, 619–626.
23. Edsjo,A. *et al*. (2003) Expression of trkB in human neuroblastoma in relation to MYCN expression and retinoic acid treatment. *Lab. Invest.*, **83**, 813–823.
24. Bordow,S.B. *et al*. (1998) Prognostic significance of MYCN oncogene expression in childhood neuroblastoma. *J. Clin. Oncol.*, **16**, 3286–3294.
25. Matsumoto,K. *et al*. (1995) Expression of brain-derived neurotrophic factor and p145TrkB affects survival, differentiation, and invasiveness of human neuroblastoma cells. *Cancer Res.*, **55**, 1798–1806.
26. Garcia-Lora,A. *et al*. (2003) MHC class I antigens, immune surveillance, and tumor immune escape. *J. Cell. Physiol.*, **195**, 346–355.
27. Koopman,L.A. *et al*. (2000) Multiple genetic alterations cause frequent and heterogeneous human histocompatibility leukocyte antigen class I loss in cervical cancer. *J. Exp. Med.*, **191**, 961–976.
28. Cromme,F.V. *et al*. (1994) Differences in MHC and TAP-1 expression in cervical cancer lymph node metastases as compared with the primary tumours. *Br. J. Cancer*, **69**, 1176–1181.
29. Andratschke,M. *et al*. (2003) MHC-class I antigen expression on micrometastases in bone marrow of patients with head and neck squamous cell cancer. *Anticancer Res.*, **23**, 1467–1471.
30. Bernards,R. *et al*. (1986) N-myc amplification causes down-modulation of MHC class I antigen expression in neuroblastoma. *Cell*, **47**, 667–674.
31. van de Stolpe,A. *et al*. (1996) Intercellular adhesion molecule-1. *J. Mol. Med.*, **74**, 13–33.
32. Fujihara,T. *et al*. (1999) Decrease in ICAM-1 expression on gastric cancer cells is correlated with lymph node metastasis. *Gastric Cancer*, **2**, 221–225.
33. Hosch,S.B. *et al*. (1997) Expression and prognostic significance of immunoregulatory molecules in esophageal cancer. *Int. J. Cancer*, **74**, 582–587.
34. Maeda,K. *et al*. (2002) Expression of intercellular adhesion molecule-1 and prognosis in colorectal cancer. *Oncol. Rep.*, **9**, 511–514.
35. Budinsky,A.C. *et al*. (1997) Decreased expression of ICAM-1 and its induction by tumor necrosis factor on breast-cancer cells *in vitro*. *Int. J. Cancer*, **71**, 1086–1090.
36. Ogawa,Y. *et al*. (1998) Expression of intercellular adhesion molecule-1 in invasive breast cancer reflects low growth potential, negative lymph node involvement, and good prognosis. *Clin. Cancer Res.*, **4**, 31–36.
37. Favrot,M.C. *et al*. (1991) Expression of leucocyte adhesion molecules on 66 clinical neuroblastoma specimens. *Int. J. Cancer*, **48**, 502–510.
38. Gross,N. *et al*. (1992) Differentiation-related expression of adhesion molecules and receptors on human neuroblastoma tissues, cell lines and variants. *Int. J. Cancer*, **52**, 85–91.
39. Foreman,N.K. *et al*. (1993) Mechanisms of selective killing of neuroblastoma cells by natural killer cells and lymphokine activated killer cells. Potential for residual disease eradication. *Br. J. Cancer*, **67**, 933–938.
40. Naganuma,H. *et al*. (1991) Increased susceptibility of IFN-gamma-treated neuroblastoma cells to lysis by lymphokine-activated killer cells: participation of ICAM-1 induction on target cells. *Int. J. Cancer*, **47**, 527–532.

41. Webb,D.S. *et al*. (1991) Cytokine-induced enhancement of ICAM-1 expression results in increased vulnerability of tumor cells to monocyte-mediated lysis. *J. Immunol.*, **146**, 3682–3686.
42. Pandolfi,F. *et al*. (1992) Expression of cell adhesion molecules in human melanoma cell lines and their role in cytotoxicity mediated by tumor-infiltrating lymphocytes. *Cancer*, **69**, 1165–1173.
43. Goodison,S. *et al*. (1999) CD44 cell adhesion molecules. *Mol. Pathol.*, **52**, 189–196.
44. Koopman,G. *et al*. (1993) Activated human lymphocytes and aggressive non-Hodgkin's lymphomas express a homologue of the rat metastasis-associated variant of CD44. *J. Exp. Med.*, **177**, 897–904.
45. Mayer,B. *et al*. (1993) De-novo expression of CD44 and survival in gastric cancer. *Lancet*, **342**, 1019–1022.
46. Wielenga,V.J. *et al*. (1993) Expression of CD44 variant proteins in human colorectal cancer is related to tumor progression. *Cancer Res.*, **53**, 4754–4756.
47. Li,H. *et al*. (1993) Variant CD44 adhesion molecules are expressed in human brain metastases but not in glioblastomas. *Cancer Res.*, **53**, 5345–5349.
48. Gross,N. *et al*. (1994) CD44H expression by human neuroblastoma cells: relation to MYCN amplification and lineage differentiation. *Cancer Res.*, **54**, 4238–4242.
49. Gao,A.C. *et al*. (1997) CD44 is a metastasis suppressor gene for prostatic cancer located on human chromosome 11p13. *Cancer Res.*, **57**, 846–849.
50. Ross,J.S. *et al*. (1996) Expression of the CD44 cell adhesion molecule in urinary bladder transitional cell carcinoma. *Mod. Pathol.*, **9**, 854–860.
51. Gross,N. *et al*. (1997) Absence of functional CD44 hyaluronan receptor on human NMYC-amplified neuroblastoma cells. *Cancer Res.*, **57**, 1387–1393.
52 Wielenga,V.J. *et al*. (1993) Expression of CD44 variant proteins in human colorectal cancer is related to tumor progression. *Cancer Res.*, **53**, 4754–4756.
53. Yamamichi,K. *et al*. (1998) Increased expression of CD44v6 mRNA significantly correlates with distant metastasis and poor prognosis in gastric cancer. *Int. J. Cancer*, **79**, 256–262.
54. Ekici,S. *et al*. (2002) Determination of prognosis in patients with prostate cancer treated with radical prostatectomy: prognostic value of CD44v6 score. *J. Urol.*, **167**, 2037–2041.

Received January 5, 2007; revised June 3, 2007; accepted June 24, 2007